

# Sign-consistent dynamical couplings between *ab initio* three-center wave functions

L. F. Errea, L. Fernández, A. Macías,\* L. Méndez, I. Rabadán,<sup>†</sup> and A. Riera

*Departamento de Química, Universidad Autónoma de Madrid, 28049 Madrid, Spain.*

*Laboratorio Asociado al CIEMAT de Física Atómica y Molecular en Plasmas de Fusión.*

(Dated: April 30, 2004)

## Abstract

We present a method to ensure the sign-consistency of dynamical couplings between *ab initio* three-center wave functions. The method also allows to systematically “diabatize” avoided crossings between two potential energy surfaces, including conical intersections. Illustrations are presented for  $\text{H}_3^+$ ,  $\text{LiH}_2^+$  and  $\text{NH}_2^5+$  quasimolecules.

---

\*Also at Instituto de Estructura de la Materia CSIC, Serrano 113 bis, 28006 Madrid, Spain.

<sup>†</sup>Electronic address: [Ismanuel.Rabadan@uam.es](mailto:Ismanuel.Rabadan@uam.es)

## I. INTRODUCTION

The theoretical treatment of atom (ion)-atom (molecule) collisions, at low energies, is usually carried out by employing a molecular expansion (see e.g. [1]) of the collisional wave function in terms of the electronic wave functions of the (quasi)molecule formed by the colliding systems. This method involves a first step where one solves the clamped-nuclei electronic equation in the Born-Oppenheimer approximation to obtain the adiabatic molecular functions (MFs) and potential energy surfaces (PES). Excitation and charge transfer processes then take place through non-adiabatic transitions between the Born-Oppenheimer states, induced by the dynamical or non-adiabatic coupling terms. Also, non-adiabatic transitions are relevant in reactive processes (e.g. F+H<sub>2</sub> reaction [2, 3]). PES and couplings are the required input of the dynamical calculation in both quantal and semiclassical formalisms.

The calculation of MFs may require large configuration interaction (CI) expansions and the evaluation of non-adiabatic couplings is an important practical aspect for which numerical and analytical techniques have been proposed (see [4] and references therein) and implemented [5–7]. These couplings can then be modified, by the inclusion of translation factors [8] (or reaction coordinates in quantal formalisms [9, 10]), to ensure that the expansion fulfills the appropriate boundary conditions (see e.g. [11, 12]).

In the present paper we address an important practical drawback of the method that is the erratic sign of the calculated dynamical couplings, which results in that one cannot directly use them in the dynamical calculations: these couplings show, in general, unphysical teeth-saw shapes because the overall sign of the MFs is arbitrary; indeed, it depends on the numerical diagonalization procedure of the Hamiltonian matrix. In practice, this usually entails a cumbersome study of the couplings and the coefficients of the MFs to ensure a consistent sign. In this paper we shall describe a method that we have implemented, and that goes a long way towards solving the problem. This method is based on the use of the delayed overlap matrix (DOM), whose elements are overlaps between the MFs at neighbor points of a grid of internuclear distances.

A second practical aspect, which is related to the sign consistency problem, is the presence of narrow avoided crossings between potential energy curves, where the adiabatic MFs vary rapidly and one of them changes sign; accordingly, the signs of some couplings change in the avoided crossing regions. This sign change is physically relevant and may be erroneously

attributed to an arbitrary change in the MFs.

A third related aspect is that in dynamical treatments one often employs an alternative diabatic basis. In this respect, several definitions of diabatic states have been proposed (see e.g. [13] and references therein), and we shall concentrate in this paper on the application of the abovementioned DOM procedure to decide whether it is convenient to “diabatize” a particular avoided crossing. It must be noted that our numerical method does not yield a physical criterion on which avoided crossings must be traversed diabatically (this depends on the collision energy and on the particular process under study); rather, its aim is to ascribe consistent signs to the MFs both in adiabatic and diabatic bases. In some cases, the use of a diabatic basis is indispensable, as when the mechanism involves a single MF whose PES shows very narrow avoided crossings with those of a series of states. An example is the  $\text{N}^{5+} + \text{H}_2$  collision [14], which is treated by constructing a diabatic MF whose PES crosses other series which may or may not be included in the expansion. We shall show the usefulness of this DOM procedure to treat this kind of situations.

For triatomics, the application of the molecular method requires to take into account the vibro-rotational motion (see reviews in Refs. [15, 16]). At the impact energies where non-adiabatic transitions take place, molecular rotation is often described in the framework of the sudden approximation, where the transition probabilities and cross sections are obtained by averaging over the relative orientation of the internuclear vector of the diatomic (see Ref. [17]). For the vibrational motion, and at low energies, a close-coupling expansion in terms of vibronic functions is required, while at higher  $E$  ( $E \geq 250$  eV/amu) [18], simplified methods based on the use of the sudden approximation can be applied. In all cases, from the computational point of view, this involves the calculation of MFs and PES in a grid of points  $(R_i, \rho_j, \alpha_k)$ , where  $\mathbf{R}$  is the ion-diatom relative vector,  $\boldsymbol{\rho}$  the diatom internuclear vector and  $\alpha$  the angle between  $\mathbf{R}$  and  $\boldsymbol{\rho}$  (Fig. 1). As an example, quantum chemistry calculations required for  $\text{He}^{2+} + \text{H}_2$  collisions have been recently presented in Ref. [19], including a diabatization of series of avoided crossings between the PES. It was then necessary to ensure that the sign is consistent over the grid  $\{(R_i, \rho_j, \alpha_k)\}$ .

A singular aspect of the three-center systems is the presence of conical intersections between the energy surfaces, which have been considered in many publications (see [13] and references therein). In particular, they are often found in the limit  $\alpha = 0$  (and  $\alpha = \pi/2$  for homonuclear targets), where the symmetry of the system increases from  $C_s$  to  $C_{\infty v}$  (or  $C_{2v}$ )

and some avoided crossings become crossings. The shapes of the dynamical couplings near a conical intersection have been illustrated in Refs. [20] and [21], where it is shown that a diabatic basis is required to eliminate the singular couplings.

The paper is organized as follows: In section II we summarize the basic definitions and the dynamical methods for ion-diatom collisions. In section III we present our method to ensure the sign consistency of the MFs, and in section IV we explain the diabatization procedure. Additional illustrations are presented in section V showing the workings of the method in the treatment of a series of avoided crossings with our example of  $\text{N}^{5+} + \text{H}_2$ .

## II. BASIC EQUATIONS

In a molecular treatment of ion-atom and ion-molecule collisions, the collisional wave function is expanded in terms of MFs,  $\Phi_l$ , which are (approximate) solutions of the Born-Oppenheimer electronic equation:

$$H_{\text{elec}}\Phi_l(\mathbf{q}; \mathbf{Q}) = E_l(\mathbf{Q})\Phi_l(\mathbf{q}; \mathbf{Q}) \quad (1)$$

where  $H_{\text{elec}}$  is the clamped-nuclei electronic Hamiltonian,  $\mathbf{q}$  and  $\mathbf{Q}$  denote electronic and nuclear coordinates, respectively, and  $E_l(\mathbf{Q})$  are the PES. In particular, for the three-center case,  $E_l(R, \rho, \alpha)$  (see Fig. 1). To solve this equation, one often employs the well known configuration interaction method (CI), in which the system wave function is expanded as a linear combination of configurations,  $\psi_j$ :

$$\Phi_l(\mathbf{q}; \mathbf{Q}) = \sum_j c_{jl}\psi_j(\mathbf{q}; \mathbf{Q}) \quad (2)$$

Here, the coefficients  $c_{jl}$  are obtained variationally from the secular equation:

$$(\mathbf{H}_{\text{elec}} - E\mathbf{\Delta})\mathbf{C} = 0 \quad (3)$$

with  $\mathbf{H}_{\text{elec}}$  and  $\mathbf{\Delta}$  the Hamiltonian and overlap matrices, whose elements are  $H_{ij} = \langle \psi_i | H_{\text{elec}} | \psi_j \rangle$  and  $\Delta_{ij} = \langle \psi_i | \psi_j \rangle$ . The electronic configurations  $\psi_j$  are spin- and symmetry- adapted, antisymmetrized products of molecular spin-orbitals ( $\phi_m$ )

$$\psi_j(\mathbf{q}; \mathbf{Q}) = \sum_k d_{jk} \mathcal{A}(\phi_{i_1}, \dots, \phi_{i_n})_k \quad (4)$$

where  $\mathcal{A}$  is the antisymmetrization operator and  $k$  is an index that denotes a given product of molecular spin orbitals. In our illustrations, we have applied a multireference CI

method, where the molecular orbitals have been obtained by means of SCF calculations. The collisional wave function is then written as a linear combination of the MFs:

$$\Psi(\mathbf{Q}, \mathbf{q}) = \sum_l F_l(\mathbf{Q}) \Phi_l(\mathbf{q}; \mathbf{Q}) \quad (5)$$

where  $F_l(\mathbf{Q})$  are calculated by substituting the expansion (5) in the corresponding full (dynamical) Schrödinger equation, yielding a set of differential equations that are solved numerically. Transitions between molecular states are induced by non-adiabatic couplings, which are the matrix elements of the nuclear gradient operator  $\nabla_{\mathbf{Q}}$ :

$$M_{lm} = \langle \Phi_l(\mathbf{q}; \mathbf{Q}) | \hat{\mathbf{X}} \cdot \nabla_{\mathbf{Q}} | \Phi_m(\mathbf{q}; \mathbf{Q}) \rangle \quad (6)$$

where  $\hat{\mathbf{X}}$  is a unit vector in any direction of  $\mathbf{Q}$ -space.

In practice, the PES and couplings are evaluated in a set of nuclear geometries  $\{\mathbf{Q}_i, \dots, \mathbf{Q}_N\}$ , and they are then interpolated at the points needed to numerically solve the system of differential equations for the functions  $F_l(\mathbf{Q})$ . In these interpolation nodes, the couplings can be evaluated numerically to first order in  $\delta$ , by taking

$$M_{lm}(\mathbf{Q}_i) = \delta^{-1} \langle \Phi_l(\mathbf{q}; \mathbf{Q}_i) | \Phi_m(\mathbf{q}; \mathbf{Q}_i + \delta \hat{\mathbf{X}}) \rangle + \mathcal{O}(\delta^2) \quad (7)$$

The dynamical couplings are then expressed in terms of the DOM between two nearby points,  $\mathbf{Q}_i$  and  $\mathbf{Q}_i + \delta \hat{\mathbf{X}}$ , which can be evaluated, by modifying the codes (see [6]), using the first order transition density matrix ( $\mathbf{D}^{lm}$ ) between these two points [22]:

$$\langle \Phi_l(\mathbf{q}; \mathbf{Q}_i) | \Phi_m(\mathbf{q}; \mathbf{Q}_i + \delta \hat{\mathbf{X}}) \rangle = n^{-1} \text{Tr}(\mathbf{D}^{lm} \mathbf{S}^*) \quad (8)$$

where  $\mathbf{S}^*$  is the corresponding DOM in the molecular orbital basis set, and  $n$  the number of electrons of the system.

To calculate the dynamical couplings of Eq. (7), we need to solve Eq. (3) at two different grid points:  $\mathbf{Q}_i$  and  $\mathbf{Q}_i + \delta \hat{\mathbf{X}}$ . If one employs a basis of real functions, both  $-\Phi_l$  and  $\Phi_l$  are solutions of Eq. (1), which means that the sign of  $\Phi_l(\mathbf{q}; \mathbf{Q})$  is arbitrary, leading to arbitrary signs of the matrix elements  $M_{lm}(\mathbf{Q}_i)$ . This arbitrariness can be corrected by calculating the diagonal elements of the DOM:

$$O_l(\mathbf{Q}_i) = \langle \Phi_l(\mathbf{q}; \mathbf{Q}_i) | \Phi_l(\mathbf{q}; \mathbf{Q}_i + \delta \hat{\mathbf{X}}) \rangle = k_l + \mathcal{O}(\delta^2) \quad (9)$$

where  $\mathbf{k}$  is a vector whose components are either +1 or -1 depending on the relative signs of the MF  $\Phi_l$  at  $\mathbf{Q}_i$  and  $\mathbf{Q}_i + \delta\hat{\mathbf{X}}$ . Therefore, we can eliminate the arbitrariness in the sign of the coupling by taking a corrected, locally sign consistent, coupling:

$$M_{lm}^s(\mathbf{Q}_i) = k_m M_{lm}(\mathbf{Q}_i) \quad (10)$$

### III. SIGN CONSISTENCY

The procedure explained above only ensures that dynamical couplings between different electronic states are sign consistent at a given nuclear geometry,  $\mathbf{Q}_i$ . Now, we are interested in obtaining sign consistent couplings in a set of nuclear geometries defining a path or a domain of nuclear configurations. For this purpose, we construct a new set of sign-consistent molecular states  $\{\Phi_j^c\}$ , as explained below.

Let  $\{\mathbf{Q}_1, \dots, \mathbf{Q}_N\}$  be an ordered grid of points along a given path in the nuclear configuration space, where the set of adiabatic molecular states  $\{\Phi_j\}$  are known. We assume that the erratic sign of  $\Phi_j$  can only arise in the CI step. That is assured by dividing the interval  $[\mathbf{Q}_i, \mathbf{Q}_{i+1}]$  in subintervals  $[\mathbf{Q}'_s, \mathbf{Q}'_{s+1}]$  (of lengths, say of about  $0.01 a_0$ ) and repeating the fast SCF calculation in the set of points  $\{\mathbf{Q}'_s\}$ ; this allows to obtain sign consistent molecular orbitals at all grid points by comparing their coefficients.

The first step is the evaluation of the DOM:

$$O_{jj}(\mathbf{Q}_i) = \langle \Phi_j(\mathbf{Q}_{i-1}) | \Phi_j(\mathbf{Q}_i) \rangle \quad (11)$$

with  $i = 2, \dots, N$ . Since we do not need an accurate value of the DOM of (11), which will be then rounded off to 0 or  $\pm 1$ , we can employ the first order expression (8) in its evaluation.

Next, we define  $n_i(j, j)$  from the following mapping:

$$\begin{cases} n_i(j, j) = 0 & \text{if } |O_{jj}(\mathbf{Q}_i) - 1| < \epsilon_1 \\ n_i(j, j) = 1 & \text{if } |O_{jj}(\mathbf{Q}_i) + 1| < \epsilon_1 \\ n_i(j, j) = 2 & \text{otherwise} \end{cases} \quad (12)$$

where  $\epsilon_1$  is a given threshold (0.2 in our calculations). In these expressions,  $n_i(j, j) = 0$  means that the state  $\Phi_j$  does not change sign when going from  $\mathbf{Q}_{i-1}$  to  $\mathbf{Q}_i$ , while  $n_i(j, j) = 1$  implies that there was a change of sign. In either case, we define a new MF  $\Phi_j^c$  by taking:

$$\Phi_j^c(\mathbf{Q}_i) = (-1)^{n_i(j, j)} \Phi_j(\mathbf{Q}_i) \quad (13)$$

On the other hand,  $n_i(j, j) = 2$  may indicate that there is an avoided crossing between the energy of  $\Phi_j$  and some other state,  $\Phi_{j'}$ , in the path from  $\mathbf{Q}_{i-1}$  to  $\mathbf{Q}_i$ . To check this possibility, we calculate the delayed overlaps with “energetically-near” states:

$$O_{jj'}(\mathbf{Q}_i) = \langle \Phi_j(\mathbf{Q}_{i-1}) | \Phi_{j'}(\mathbf{Q}_i) \rangle \quad (14)$$

which leads, for each  $j'$ , to the mapping  $n_i(j, j')$ :

$$\begin{cases} n_i(j, j') = 0 & \text{if } |O_{jj'}(\mathbf{Q}_i) - 1| < \epsilon_1 \\ n_i(j, j') = 1 & \text{if } |O_{jj'}(\mathbf{Q}_i) + 1| < \epsilon_1 \\ n_i(j, j') = 2 & \text{otherwise} \end{cases} \quad (15)$$

If  $n_i(j, j') \neq 2$  for some  $j'$ , we proceed to “diabatize” the crossing:

$$\phi_j^c(\mathbf{Q}_i) = (-1)^{n_i(j, j')} \phi_{j'}(\mathbf{Q}_i) \quad (16)$$

This means that the energies of MFs  $j$  and  $j'$  must be exchanged when going from  $\mathbf{Q}_{i-1}$  to  $\mathbf{Q}_i$ . Incidentally, Eq. (16) is directly applied when it is necessary to “diabatize” unphysical avoided crossings that are a consequence of employing a subgroup of the molecular point group, so that real crossings can appear as sharp pseudocrossings in the calculation. For example,  $C_s$  symmetry is often employed for linear configurations ( $C_{\infty v}$ ) of three-center systems, where  $\Sigma$  and  $\Delta$  configurations belongs to the  $A'$  irreducible representation. Then, one obtains in these calculations unphysical (very narrow) avoided crossings between  $\Sigma$  and  $\Delta$  states; these are crossed by applying (16).

The result  $n_i(j, j') = 2 \quad \forall j'$  indicates that  $\mathbf{Q}_i$  is too far from  $\mathbf{Q}_{i-1}$  to obtain a DOM close to 1 for some  $j'$ . In this case, we add an intermediate point to the grid and repeat the process. Also, if we obtain  $n_i(j, j') \neq 2$  and we do not want to traverse diabatically the  $j - j'$  avoided crossing, additional points must be included in the interval  $[\mathbf{Q}_{i-1}, \mathbf{Q}_i]$  in order to follow smoothly the adiabatic states.

In the new  $\{\Phi_j^c\}$  basis, the corrected couplings  $M_{lm}^c(\mathbf{Q}_i)$ , sign-consistent with those at  $\mathbf{Q}_{i-1}$ , are:

$$M_{lm}^c(\mathbf{Q}_i) = (-1)^{n_i(l, l') + n_i(m, m')} M_{l'm'}^s(\mathbf{Q}_i) \quad (17)$$

where  $l'$  and  $m'$  are those for which  $n_i$  is either 0 or 1.

In ion-molecule collisions, the required dynamical couplings are the radial ( $\langle \Phi_l | \partial \Phi_m / \partial R |_{\rho, \alpha} \rangle$ ), rotational ( $\langle \Phi_l | \partial \Phi_m / \partial \alpha |_{R, \rho} \rangle$ ) and vibrational

( $\langle \Phi_l | \partial \Phi_m / \partial \rho |_{R,\alpha} \rangle$ ) ones. In Fig. 2, we consider, as a benchmark example, radial and rotational couplings (panels (b) and (c), respectively) between the two first  $^1A'$  MFs of  $H_3^+$  along the path with  $\rho = 1.4 a_0$ ,  $\alpha = 60^\circ$  and  $1 \leq R \leq 8$ , where the corresponding PES do not show any avoided crossing (panel (a)). Along this path, we find that  $n_i(j, j) \neq 2$  for  $j = 1, 2$  and  $\forall i$ . We can see that the original couplings (symbols) jump erratically, while those in the  $\{\Phi^c\}$  basis (13) (solid lines) are perfectly smooth.

#### IV. DIABATIZATION

We now consider the diabaticization of a physical avoided crossing. As usual, we start from the crossing between the energies of two diabatic states  $\{\Phi_1^d, \Phi_2^d\}$  and perform the well known Smith rotation [23, 24]:

$$\begin{pmatrix} \Phi_1^d \\ \Phi_2^d \end{pmatrix} = \begin{pmatrix} \cos \theta & -\sin \theta \\ \sin \theta & \cos \theta \end{pmatrix} \begin{pmatrix} \Phi_1^c \\ \Phi_2^c \end{pmatrix} \quad (18)$$

where  $\{\Phi_1^c, \Phi_2^c\}$  are adiabatic states. This yields the well known expression for the transformation angle:

$$\theta = \frac{\pi}{4} + \frac{1}{2} \tan^{-1} \left( \frac{H_{22}^d - H_{11}^d}{2H_{12}^d} \right) \quad (19)$$

where  $H_{ij}^d = \langle \Phi_i^d | H_{\text{elec}} | \Phi_j^d \rangle$ . The energies of the diabatic states cross at  $R = R_0$ . Following the analysis of Ref. [21, 25], for each  $\rho$ , and near the avoided crossing, we approximate  $H_{22}^d - H_{11}^d$  by a linear (in  $R$ ) expression, while the interaction term  $H_{12}$  is assumed independent of  $R$ :

$$H_{22}^d - H_{11}^d = R - R_0 \quad (20)$$

$$2H_{12}^d = \gamma \quad (21)$$

Here, both  $R_0$  and  $\gamma$  vary with  $\alpha$ .

Differentiation of eqs. (18) and (19) leads to:

$$\langle \Phi_1 | \left. \frac{\partial}{\partial R} \right|_{\alpha, \rho} | \Phi_2 \rangle - \langle \Phi_1^d | \left. \frac{\partial}{\partial R} \right|_{\alpha, \rho} | \Phi_2^d \rangle = -\frac{1}{2} \frac{\gamma}{\gamma^2 + (R - R_0)^2} \quad (22)$$

$$\langle \Phi_1 | \left. \frac{\partial}{\partial \alpha} \right|_{R, \rho} | \Phi_2 \rangle - \langle \Phi_1^d | \left. \frac{\partial}{\partial \alpha} \right|_{R, \rho} | \Phi_2^d \rangle = \frac{1}{2} \frac{\gamma}{\gamma^2 + (R - R_0)^2} \left( \frac{(R - R_0)}{\gamma} \frac{\partial \gamma}{\partial \alpha} + \frac{\partial R_0}{\partial \alpha} \right) \quad (23)$$

To illustrate the application of the model of Eqs. (22) and (23), we show in Fig. 3 an example corresponding to an avoided crossing between the energies of states  $5^1A'$  and  $6^1A'$  of  $\text{H}_3^+$  ( $\rho = 2.06 a_0$  and  $\alpha = 60^\circ$ ). We have plotted in the panel (a) of this figure the energies of these two states, and in panel (b) the calculated radial and rotational couplings (symbols) in the adiabatic sign consistent  $\{\Phi_i^c\}$  representation. The solid symbols in the panel (b) correspond to a sparse distribution of grid points along  $\mathbf{R}$ . In order to treat this avoided crossing one has two options: to employ the adiabatic basis or to diabaticize the crossing. The first option involves the integration of the couplings along  $\mathbf{R}$  and requires a dense mesh of grid points near the avoided crossing where the couplings vary rapidly. The second option involves the transformation to a diabatic basis set  $\{\Phi_i^d\}$  using Eqs. (18) and (19). In this basis, the interaction matrix element  $\langle \Phi_1^d | H_{\text{elec}} | \Phi_2^d \rangle$ , which is easily obtained, varies smoothly through the crossing region and, for narrow avoided crossings, can often be neglected at not too low collision energies. Moreover, the dynamical couplings are smooth in the diabatic basis, which allows us to employ a scarce mesh of grid points for the dynamical calculation in this basis. Also, the couplings of the diabatic states  $\{\Phi_1^d, \Phi_2^d\}$  with the rest of states  $\Phi_j^c$ , not involved in the crossing, are easily related to those in the adiabatic basis by means of Eq. (18).

To define the diabatic set, we can fit to Eqs. (22) and (23) the couplings in the adiabatic basis, evaluated in a sparse grid of points. In this fitting procedure we assume that the couplings between the diabatic states are constant in the avoided crossing region. This is shown in Fig. 3, where the solid lines are the result of fitting the couplings evaluated at the points indicated by solid symbols. The couplings at the intermediate points, indicated by open symbols, were calculated afterwards to test the precision of the model.

Conical intersections can be treated as particular cases of Eq. (19). Explicitly, for a conical intersection at  $\alpha = \alpha_0$  ( $\alpha_0 = 0$  or  $\pi/2$ ),  $\gamma(\alpha)$  can be approximated, near the conical intersection, by

$$\gamma(\alpha) \simeq \gamma_0 |\alpha - \alpha_0| \quad (24)$$

In this case, eq. (23) reduces to:

$$\begin{aligned} & \langle \Phi_1 | \frac{\partial}{\partial \alpha} \Big|_{R,\rho} | \Phi_2 \rangle - \langle \Phi_1^d | \frac{\partial}{\partial \alpha} \Big|_{R,\rho} | \Phi_2^d \rangle = \\ & \frac{1}{2} \frac{\gamma_0 (R - R_0) \text{sign}(\alpha - \alpha_0)}{\gamma_0^2 (\alpha - \alpha_0)^2 + (R - R_0)^2} \end{aligned}$$

$$+\frac{1}{2} \frac{\gamma_0 |\alpha - \alpha_0|}{\gamma_0^2 (\alpha - \alpha_0)^2 + (R - R_0)^2} \frac{\partial R_0}{\partial \alpha} \quad (25)$$

The first term of the right hand side of (25), which becomes a pole in the limit  $\alpha \rightarrow \alpha_0$  [21, 25], decreases rapidly when  $|\alpha - \alpha_0|$  increases. The second term of this equation, which is negligible for  $\alpha \rightarrow \alpha_0$  is a Lorentzian-type term similar to that of (22).

In practice, our procedure involves, first, a calculation of the DOM, and secondly, application of Eqs. (13) and (16) to obtain sign consistent molecular wave functions, and “diabatizing” avoided crossings whose DOM values are smaller than the threshold  $\epsilon_1$ . If necessary, one can then incorporate an additional procedure to properly diabatize the crossings using the transformation (18). This involves a fitting of the derivative couplings in the avoided crossing region to expressions (22) and (23), to determine the parameters  $R_0$ ,  $\gamma$ ,  $\frac{\partial R_0}{\partial \alpha}$  and  $\frac{\partial \gamma}{\partial \alpha}$ , usually assuming that the couplings  $\langle \Phi_1^d | \frac{\partial}{\partial \alpha} |_{R,\rho} | \Phi_2^d \rangle$  and  $\langle \Phi_1^d | \frac{\partial}{\partial R} |_{\alpha,\rho} | \Phi_2^d \rangle$  are negligible with respect to those in the adiabatic basis.  $R_0$  and  $\gamma$  are non-linear parameters and their fitting is delicate. Our procedure begins by finding an initial guess for  $R_0$  (from the approximate crossing point of the corresponding energies) and  $\gamma$ , solving Eq. (22), with the approximate value of  $R_0$ , at two consecutive grid points next to  $R_0$ , and taking the common root. Then, any non-linear fitting routine with initial guess should work properly with Eq. (22). On the other hand, the linear parameters  $\partial R_0 / \partial \alpha$  and  $\partial \gamma / \partial \alpha$  are easily obtained by fitting (23) with a standard least-squared method. In the fittings we use only four points; two at each side of the avoided crossing.

Our second illustration shows the variation of the PES and couplings, corresponding to an avoided crossing of  $\text{LiH}^{2+}$ , with respect to changes in the angle  $\alpha$ . In particular, we have plotted in Fig. 4 the energy differences, radial and rotational couplings between the second and third  ${}^1A'$  states of  $\text{LiH}_2^+$  for several angles. These two states correlate to  $\text{H}^+ + \text{LiH}(X^1\Sigma^+)$  and  $\text{H}(1s) + \text{LiH}^+(2^2\Sigma^+)$  as  $R$  increases. One can note in this figure that there is an avoided crossing that becomes wider as  $\alpha$  decreases. Here we have employed the adiabatic representation, and we have fitted the couplings to expressions (22) and (23) to show the usefulness of the model. The values obtained for the fitted parameters  $R_0$ ,  $\gamma$ ,  $\partial R_0 / \partial \alpha$  and  $\partial \gamma / \partial \alpha$  are shown in Fig. 5 as a function of  $\alpha$ . In this example,  $\frac{\partial R_0}{\partial \alpha}$  is not negligible, which leads to a dominant contribution of the second term of Eq. (25) to the rotational coupling, and this produces its unusual delta-like peak near the avoided crossing region. For  $\alpha = 180^\circ$ , the nuclear geometry is collinear with the nuclei ordered H-Li-H and,

when the hydrogen nuclei are equidistant to Li, the avoided crossing becomes a symmetry induced conical intersection between  ${}^1\Sigma_g^+$  and  ${}^1\Sigma_u^+$  states.

## V. SERIES OF AVOIDED CROSSINGS.

The use of automatic sign consistent procedures is very useful when one has to deal with multiple crossings where “diabatization” is indispensable. As an illustration, we consider the collision of  $\text{N}^{5+}$  with  $\text{H}_2$  that we have studied in detail in Ref. [14]. In that paper, it is explained that the PES of the entrance and main exit channels lie above four Rydberg series, and a block-diagonalization technique is required to evaluate these PES and the corresponding couplings. After applying the procedure of section III, we obtained the PES of Fig. 6, where we plot the energies (for  $\alpha = 45^\circ$  and  $\rho = 1.4 a_0$ ) of the first 30 excited MFs of symmetry  ${}^1A'$ , relative to that of the ground state, that dissociates in the limit  $R \rightarrow \infty$  into  $\text{N}^{4+}(3s)+\text{H}_2^+(X^2\Sigma_g^+)$ .

The thick line in Fig. 6 is the energy of the collisional entrance channel, which correlates to  $\text{N}^{5+}(1s^2)+\text{H}_2(X^1\Sigma_g^+)$ ; this energy shows avoided crossings for  $R > 6 a_0$  with those of other single and double capture states, and we shall concentrate on the set of avoided crossings with the energies of the MFs correlating to  $\text{N}^{3+}(3s3l)+\text{H}^++\text{H}^+$ , shown in the inset of the figure, where we have indicated the grid of  $R$ -values of our calculation. These avoided crossings are so sharp that an adiabatic treatment would require a huge number of grid points. Accordingly, we have build up a diabatic basis using Eqs. (13) and (16) with  $\epsilon_1 = 0.2$ , which leads to the diabatic energies shown in Fig. 6.

To illustrate the couplings between one MF involved in the series of crossings and other states, we plot in Fig. 7 the radial couplings (absolute values) of the adiabatic states of the inset of Fig. 6 with the ground state of our calculation (solid symbols). We have also plotted the coupling between the ground state and the diabatic entrance channel (number 8 in Fig. 6), which shows that a smooth radial coupling is obtained by simply applying Eqs. (13) and (16). In this example, the radial couplings in the adiabatic basis between the entrance channel and the states of the series correlating to  $\text{N}^{3+}(3s3l)+\text{H}^++\text{H}^+$  have delta-like peaks. In such a case, it is sufficient to use the “diabatization” procedure of (15) to eliminate the peaks and to obtain smooth couplings in the new basis (see Fig. 7).

Rotational couplings are also corrected applying the procedure of section III. This can

be seen in Fig. 8, where we have plotted in panel (a) the original couplings (solid symbols) between the states of the inset of Fig. 7, and in panel (b) the corrected couplings (open symbols) in the “diabatized” basis set  $\{\Phi_i^c\}$  between states 9, 10 and 11. In panel (b), it can be appreciated that corrected couplings are composed out of many jumps between different couplings in the adiabatic basis (here plotted only magnitude and multiplied by  $-1$ ).

Incidentally, if a grid point happens to be very close to the maximum of a given peak, then, small absolute values of the DOM are obtained for the states involved in the avoided crossing. In this case, it is more convenient to remove this point or to move it, in order to obtain higher values of  $O_{jj'}$ .

## VI. CONCLUDING REMARKS.

We have presented a practical method to evaluate sign-consistent dynamical couplings. Our use of the term “sign-consistent” implies that couplings calculated at grid points would evolve into continuous functions as the distance between the grid points is progressively diminished. An obvious exception occurs when the adiabatic couplings must be discontinuous: a well-known instance takes place in the neighborhood of conical intersections [26]; there, most couplings are continuous functions for any closed path except at a single point, where they change sign. In this case our procedure yields the same behavior.

The method is based on the use of the DOM, which is easily evaluated by extending the numerical techniques applied to obtain the couplings, and the method is implemented for multireference CI wave functions. Since we are interested in determining the relative sign of the wave functions in two grid points, accurate values of the DOM are not required, which allows us to employ numerical first order differentiation. The method is particularly useful in the neighbourhood of avoided crossings between the PES, where it is necessary to distinguish between physical (due to the avoided crossing) and unphysical sign changes. It is important to note that series of avoided crossings appear in practically all ion-molecule collisions, where the PES of a given MF (usually the collision entrance channel) shows many avoided crossings with other surfaces. Although a qualitative description of the collision is simple in terms of diabatic states, and the construction of the corresponding diabatic surfaces can be carried out by smoothly joining the adiabatic ones, a systematic method to assign consistent signs to the diabatic MFs is required when they are used in dynamical

calculations.

The procedure depends on some parameters ( $\epsilon_1$ , and the distance between grid points) which are at the users' disposition. By choosing then, he/she can obtain the sign-consistent dynamical coupling between the adiabatic states or the residual sign-consistent term between partially diabatic states. It is possible that, in order to decide which issue is more convenient in an actual calculation, the user needs to perform calculations with different parameters. We note that, in this respect, an asset of the method is that it is not 100% automatic and relies on the users' criteria. This is why we state in the introduction that the method goes a long way to "solving the problem", since the problem depends on the situation and what is required.

The workings of our method have been illustrated for three-center systems:  $\text{H}_3^+$ , as a benchmark system,  $\text{LiH}_2^+$ , as an example of a system with a marked anisotropy, and  $\text{NH}_2^{5+}$ , where a closely knit series of avoided crossings appear.

## ACKNOWLEDGMENTS

This work has been partially supported by DGICYT projects BFM2000-0025 and FTN2000-0911. IR acknowledges MCyT for a "Ramón y Cajal" contract.

- 
- [1] B. H. Bransden and M. H. C. McDowell, *Charge Exchange and the Theory of Ion-Atom Collisions* (Oxford: Clarendon, 1992).
  - [2] T.-X. Xie, Y. Zhang, M.-Y. Zhao, and K.-L. Han, *Phys. Chem. Chem. Phys.* **5**, 2034 (2003).
  - [3] M. H. Alexander, D. E. Manolopoulos, and H.-J. Werner, *J. Chem. Phys.* **113**, 11084 (2000).
  - [4] A. Macías and A. Riera, *Phys. Rep.* **81**, 299 (1982).
  - [5] R. J. Buenker, S. D. Peyerimhoff, and P. J. Bruna, *Computational Theoretical Organic Chemistry*, Ed. I. G. Csizmadia and R. Daudel (Dordrecht:Reidel, 1981).
  - [6] J. F. Castillo, L. F. Errea, A. Macías, L. Méndez, and A. Riera, *J. Chem. Phys.* **103**, 2113 (1995).
  - [7] *MOLPRO is a package of ab initio programs written by H. J. Werner and P. J. Knowles, with contributions from J. Almlöf, R. D. Amos, M. J. O Deegan, S. T. Elbert, C. Hampel, W. Meyer, K. Peterson, R. Pitzer, A. J. Stone, P. R. Taylor and R. Lidth..*

- [8] D. R. Bates and R. McCarroll, Proc. Roy. Soc. A **245**, 175 (1958).
- [9] M. H. Mittleman, Phys. Rev. **188**, 231 (1969).
- [10] W. R. Thorson and J. B. Delos, Phys. Rev. A **18**, 117 (1978).
- [11] L. F. Errea, A. Macías, L. Méndez, and A. Riera, in *The Physics of Multiply and Highly Charged Ions, vol 2, Edited by Fred J. Currell*, 237–274 (Kluwer Academic Publishers: Dordrecht, 2003).
- [12] R. McCarroll, in *The Physics of Multiply and Highly Charged Ions, vol 2, Edited by Fred J. Currell*, 275–308 (Kluwer Academic Publishers: Dordrecht, 2003).
- [13] M. Baer, Phys. Rep. **358**, 71 (2002).
- [14] L. F. Errea, L. Fernández, L. Méndez, A. Macías, I. Rabadán, and A. Riera, Phys. Rev. A **69**, 012705 (2004).
- [15] V. Sidis, Adv. At. Mol. Phys **26**, 161 (1990).
- [16] E. A. Gislason, G. Parlant, and M. Sizun, Advances in Chemical Physics **82**, 321–421 (1992).
- [17] L. F. Errea, J. D. Gorfinkiel, A. Macías, L. Méndez, and A. Riera, J. Phys. B: At. Mol. Opt. Phys. **30**, 3855 (1997).
- [18] L. F. Errea, A. Macías, L. Méndez, I. Rabadán, and A. Riera, Phys. Rev. A **65**, 010701(R) (2001).
- [19] L. F. Errea, A. Macías, L. Méndez, B. Pons, and A. Riera, J. Chem. Phys. **118**, 325 (2003).
- [20] W. Domcke and C. Woywod, Chem. Phys. Lett. **216**, 362 (1993).
- [21] D. Elizaga, L. F. Errea, A. Macías, L. Méndez, A. Riera, and A. Rojas, J. Phys. B: At. Mol. Opt. Phys. **32**, L697 (1999).
- [22] I. L. Cooper, J. Phys. B: At. Mol. Opt. Phys. **24**, 1517 (1991).
- [23] F. T. Smith, Phys. Rev. **179**, 111 (1969).
- [24] M. Baer, Advances in Chemical Physics **82**, 187–241 (1992).
- [25] L. F. Errea, A. Macías, L. Méndez, I. Rabadán, A. Riera, A. Rojas, and P. Sanz, Phys. Rev. A **63**, 062713 (2001).
- [26] G. Herzberg, H. C. Longuet-Higgins, Discuss. Faraday Soc. **35**, 77 (1963).

FIG. 1: Nuclear coordinates for ion-diatom collisions.

FIG. 2: (a) Energies of the first two  $^1A'$  MFs of  $\text{H}_3^+$  as functions of  $R$  for  $\rho = 1.4 a_0$  and  $\alpha = 60^\circ$  (coordinates of Fig. 1. Panels (b) and (c): radial and rotational couplings, respectively, between the states of panel (a), in the  $\{\Phi\}$  ( $\bullet$ ) and  $\{\Phi^c\}$  (solid line) representations.

FIG. 3: (a) Potential energy curves of the fifth and sixth  $^1A'$  states of  $\text{H}_3^+$  for  $\rho = 2.06 a_0$ ,  $\alpha = 60^\circ$ . (b) Radial and rotational couplings between the states of panel (a). The symbols are the calculated values in the basis  $\{\Phi_i^c\}$ , but only the solid symbols were used in fitting the couplings to the model of (22) and (23). Solid lines are the model.

FIG. 4: Energy differences (a), radial (b) and rotational (c) couplings between the MFs  $2^1A'$  and  $3^1A'$  of  $\text{LiH}_2^+$  states as functions of  $R$  (the distance from the  $\text{H}^+$  nucleus to the center of mass of the  $\text{HLi}$  molecule). The distance  $\text{H-Li}$  in the target molecule is fixed to  $3.04 a_0$ . The values of  $\alpha$  are indicated in panel (b). In panels (b) and (c), the symbols are the *ab initio* values, while the lines are the fitted model of Eqs. (22) and (23).

FIG. 5: Fitted parameters of model (19) to the *ab initio* values of Fig. 4.

FIG. 6: Potential energy curves of the first 30  $^1A'$  states of  $\text{N}^{5+} + \text{H}_2$  as functions of  $R$  with  $\rho = 1.4 a_0$  and  $\alpha = 45^\circ$ . — : entrance channel  $\text{N}^{5+}(1s^2)+\text{H}_2(1\sigma_g^2)$ ; — : double electron capture channels  $\text{N}^{3+}(3s3l)+\text{H}^++\text{H}^+$ ; — : other single and double electron capture channels. In the inset,  $+$  mark the grid points.

FIG. 7: Radial couplings between the ground state of  $\text{NH}_2^{5+}$  and those in the inset of Fig. 6. Solid symbols: radial couplings (only magnitude) before applying mapping (15), i. e. in the adiabatic basis set; open symbols, radial coupling between the entrance channel and the ground state of  $\text{NH}_2^{5+}$  after applying procedure of section III. Straight lines between solid symbols are drawn to guide the eye.

FIG. 8: Rotational couplings between some states of the inset of Fig. 6. Panel (a): original couplings before applying procedure of section III. Panel (b): selected corrected couplings (open symbols) in the basis  $\{\Phi_i^c\}$ ; also, the absolute value of the couplings of panel (a), multiplied by  $-1$ , are plotted (solid symbols). Straight lines between solid symbols are drawn to guide the eye.

Figure 1, Errea et al, J. Chem. Phys.

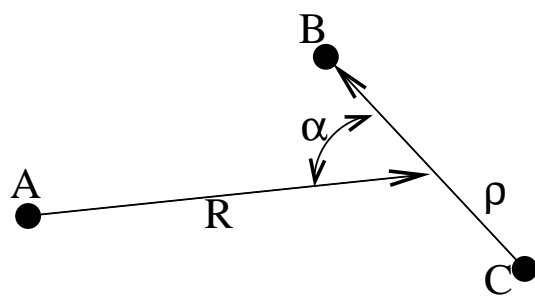


Figure 2, Errea et al, J. Chem. Phys.

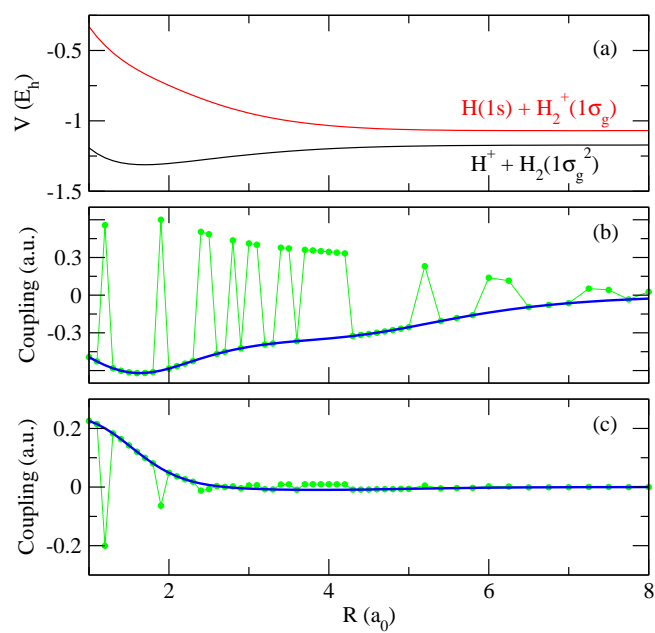


Figure 3, Errea et al, J. Chem. Phys.

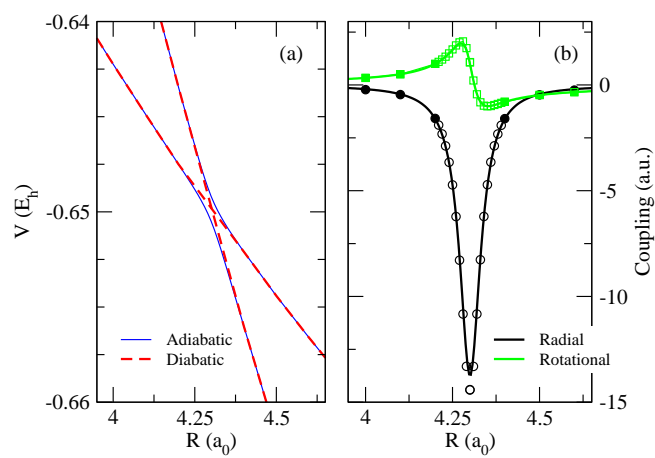


Figure 4, Errea et al, J. Chem. Phys.

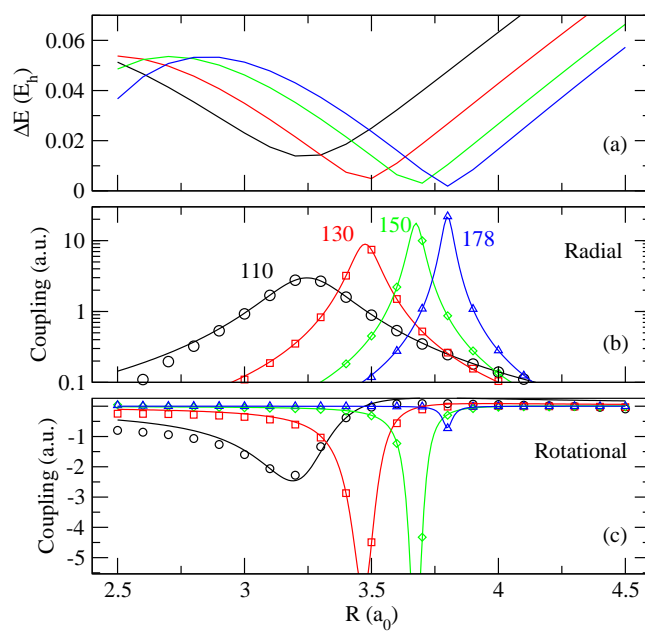


Figure 5, Errea et al, J. Chem. Phys.

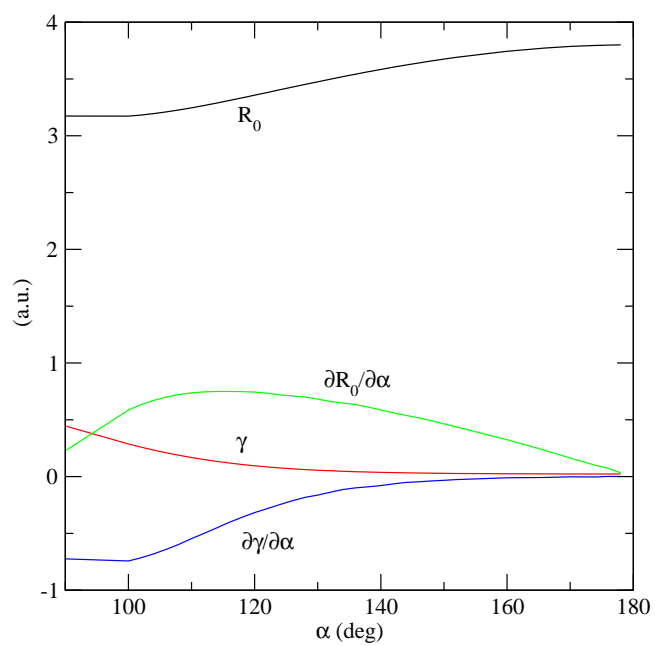


Figure 6, Errea et al, J. Chem. Phys.

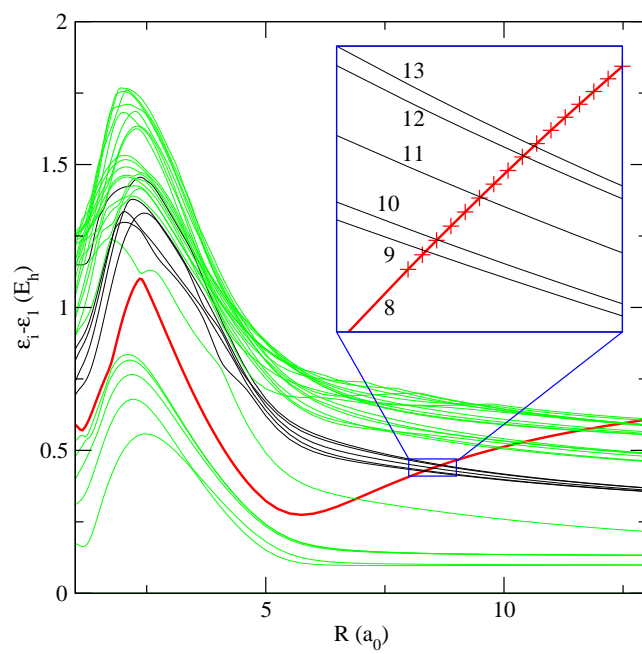


Figure 7, Errea et al, J. Chem. Phys.

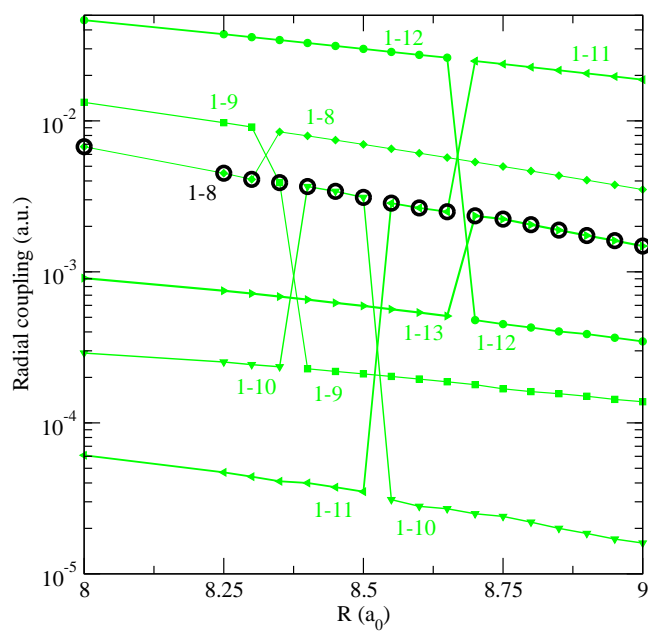


Figure 8, Errea et al, J. Chem. Phys.

